Науки о Земле
Earth sciences

Geological and petrographical studies around Um Taghir area, Central Eastern Desert, Egypt

Hamdy Ahmed Mohamed AWAD*,
Aleksey Valer`evich NASTAVKIN

Southern Federal University, Rostov-on-Don, Russia

Annotation

Um Taghir area is located in the northern extreme boundary of Central Eastern Desert of Egypt at the west of Safaga City. Um Taghir is represented by island arc related rocks and late to post tectonic magmatism. The island arc related rocks are represented by metavolcaniclastic sequences and metagabrroic rocks. Metavolcanoclastic rocks are considered as the older rock units of the study are and intruded by the metagabbro. The late to post tectonic magmatism is represented by (dokhan volcanic, gabbro, tonalite-granodiorite, monzogranite, alkali feldspar granites and different types of dikes). Usually, the gabbroic rock is bearing ilmenite lenses or bands in the bottom of the layered; this is related to magma rich of iron oxides.

Petrographically, island arc assemblage is classified in to actinolite hornblende schist and metagabbro that show quite different of their content in plagioclase, hornblende, augite, quartz and biotite. Occasionally, the late to post tectonic magmatism represented by andesite, gabbro, tonalite, granodiorite monzogranite, alkali feldspar granites and different types of dikes. Andesite consists of plagioclase, quartz, alkali feldspar and hornblende. Gabbroic rocks are represented by pyroxene hornblende gabbro and leucogabbro. They show quite different of their content in plagioclase, pyroxene and clear difference in the content of both olivine and hornblende in both of them. While tonalite and granodiorite show quite different of their content in plagioclase, quartz, hornblende, alkali felspar and biotite. On the other hand, monzogranite and alkali feldspar granite, they show plagioclase is varying from oligoclase to albite; K-feldspars, quartz and muscovite are relatively more abundant in the alkali feldspar granite. Finally, the different types of dikes classified into granite, andesite, rhyolite and basalt dikes consist of the different mineral compositions.

Keywords: Um Taghir area, petrography, Eastern Desert, Egypt.

Introduction

Um Taghir area is located in the northern extreme boundary of Central Eastern Desert of Egypt at the west of Safaga City (Fig. 1). It covers about 900 km², between longitudes 33°35′00″ and 33°50′00″ and latitudes 26°35′00″ and 26°49′00″. The area is characterized by low to relatively high topography reliefs varying from 599 to 1032 m above sea level. It forms a part of Neoproterozoic evolution of the North Arabian-Nubian Shield in the NE Africa which is belonging to the East African Orogen (EAO) as results of accretion plateaus in the course of consolidation of the Gondwana (Gass, 1982; Stern, 1994; Kröner et al., 1994; Abd Elsalam; Abd El-Wahed, I. A. Thabet, 2017; Gahlan H. A., Azer M. K., Asimow P., Al-Kahtany K., 2016; Hamimi Z., Zoheir B. A., Younis M. H., 2015 and Stern, 1996). A generalized picture shows three major organs that shaped the final configuration of greater Gondwana, whereas the East African Orogen (EAO) resulted from the collision and amalgamated arc terrains of the Arabian-Nubian Shield (ANS) with the Sahara and Congo–Tanzania crotons to the west and Azania

and Afif terrains to the east constituting one of more continent blocks between the Indian Shield and Congo–Tanzania–Bangwenla Croton (Collines and Pisarrisky, 2005). Generally, the ANS represent one largest expanses of mantle-derived, juvenile Neoproterozoic crust in the world, which is extended over 3500 km as length and more than 1500 km as width, on the other hand the part of African Orogen (EAO) of Arabian Nubian Shield is covered about 2.7 · 10⁶ km² (Johnson, 2014). Protolith rocks in the north part of ANS are middle-late Cryogenian age (~780–680 Ma), on the other hand the investigated area is belonging to the rock units crop out in the far of the northwestern part of ANS and it is related to the late Cryogenian-Ediacaran age (~690–600 Ma) (Johnson, 2014). The exposed different rock units of the study area belong to the Northern part of the Arabian-Nubian Shield (ANS) that began at ~870 Ma and established at ~620 Ma ago, when convergence between east and west Gondwana fragments closed the Mozambique ocean along the East African-Antarctic Orogen (EAAO) (Stern, 1994;
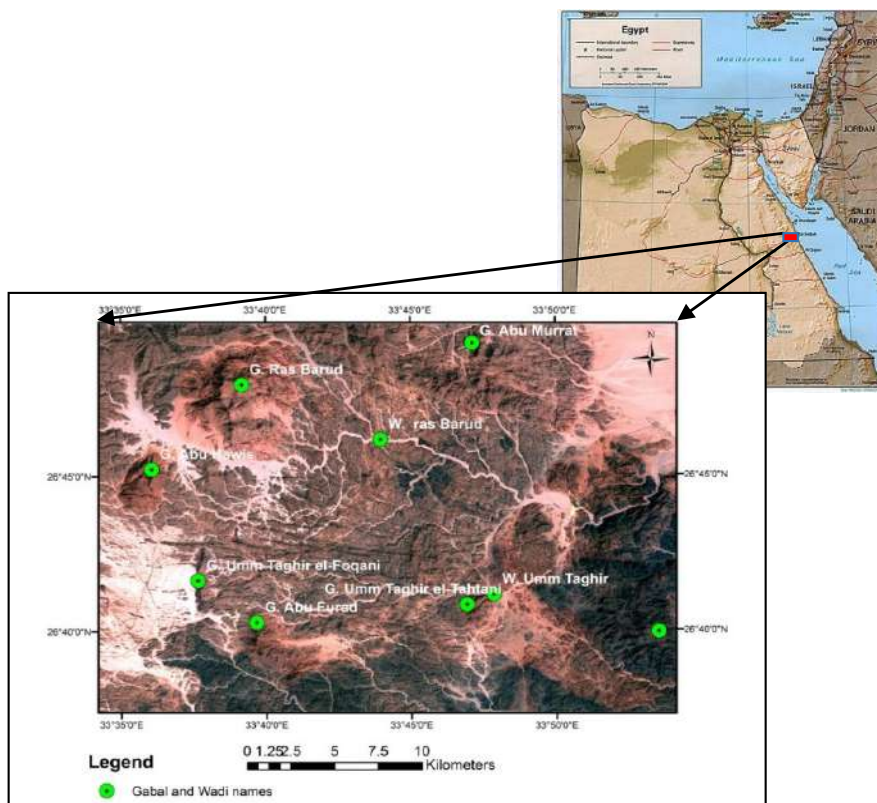
✉hamdiawaad@gmail.com
https://orcid.org/0000-0001-5306-8015
https://orcid.org/0000-0003-1472-9399

Figure 1. Sentinal-2B 421 in RGB image showing the location of the study area.
Рисунок 1. Индикатор-2B 421 в RGB-изображении, показывающий местоположение области исследования.
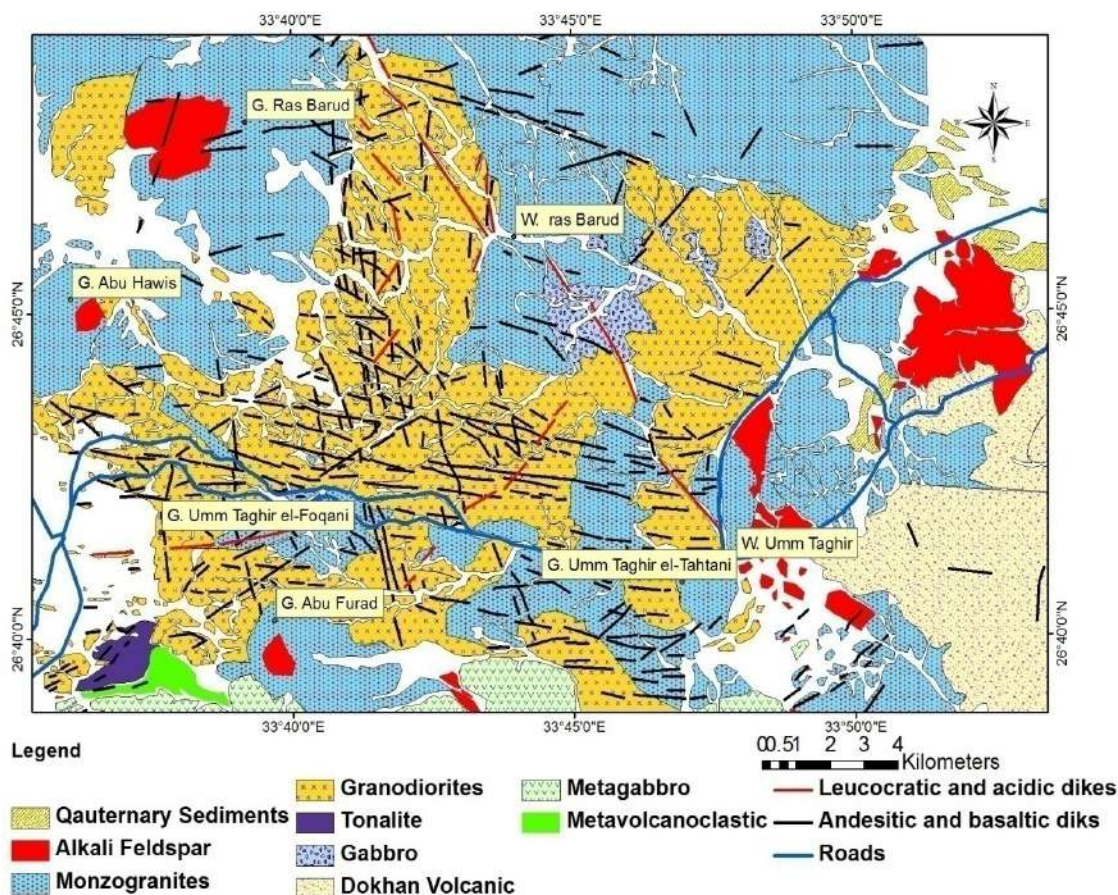

Figure 2. Simplified geological map of Um Taghir area created from integrated remotely sensed data processing and field observation.
Рисунок 2. Упрощенная геологическая карта области Ум Тагир, созданная на основе интегрированной дистанционной обработки данных и наблюдения на местах.

Jacobs and Thomas, 2004). According to the Field observations the study area is along to largest shear zone (Qena–Safaga shear zone is recognized by El Gaby et al., 1988), so the area affected by this shear zone to show metamorphic and non-metamorphic magmatic rocks are covering the study area. The metamorphic rocks are represented by the metavolcaniclastic sequences and metagabbro, while the non-metamorphic rocks are represented by Dokhan volcanic, gabbroic rocks, tonalite, granodiorite, monzogranite and alkali feldspar granite, in addition to various dikes of different composition. The resulting geologic equipment is commonly referred to as the western arc of ANS – oceanic arc terrains of ANS (Stoester and Forst, 2006; Ali et al., 2009; Johnson et al., 2011). The studied exposed rock unites are represent a part of northwestern Arabian Nubian Shield, which it is divided into two main terrains, oceanic arc terrains magmatism (metavolcaniclastic sequences and metagabbro), and followed by the continental arc terrains magmatism (late and post magmatism) as shown in Fig. 2. Several researchers have been studied Wadi Um Taghir along Qena–Safaga road (Hume, 1934; Akaad et al., 1973; 1979; Habib, 1987; El Gaby, Habib, 1982; El Gaby et al., 1988; Fowler et al., 2006, Hassan S. M., Ramadan T. M., 2014; El-Bialy M. Z., Omar M. M., 2015).

Geologic setting. The exposed rock units in this area have been differentiated into 8 distinct units (metavolcaniclastic sequences, metagabbro, dokhan volcanic, gabbro, tonalite, granodiorite, monzogranite, alkali feldspar granite and dikes) as showing in Table 1, Fig. 2.

The examined rock units are belonging to Late Cryogenian-Ediacaran age magmatism of the East African Orogeny (EAO), they are represented by Island arc assemblage (oceanic crust terrain), late to post amalgamation (continental crust terrain) (Johnson et al., 2011; Johnson, 2014).

I. Island arc assemblage. The investigated rock units of the study area are related to island arc assemblage comprise into metavolcaniclastic sequences and metagabbro and covers about 12% of the all rock volume constitution as shown in Fig. 2. Occasionally, these rocks are related to the western arc or oceanic terrains of ANS that collided and amalgamated between 680 and 640 Ma creating a new continental crustal block referred to as the proto-Arabian-Nubian Shield (pANS), (Johnson et al., 2011).

I.1. Metavolcanoclastic rocks. These rocks are considered as the older rock units of the mapped area (Fig. 2), represent about 5% of exposed rock units, and they are situated at the southern part of the study area in Gable Abu Furad (Fig. 2), they have the banded to show like schistosity bands trends to

SW direction in the most cases. Metavolcaniclastic sequences are low land, highly weathered and joints, they are intruded by the metagabbro and show sharp contact with monzogranite. They are mainly varied in color, in composition and in grain size from fine to very fine grained. The metavolcaniclastic sequences are characterized by folding structure according to elastic minerals constituents bearing in the rock and schistosity texture (Fig. 3, a).

I.2. Metagabbro. It is located at the south part of Um Taghir area and represents about 7% of exposed rock units of the study area (Fig. 2). It characterized by low hills to moderate relief out crops relative to the surrounded other rock units. Generally, this metagabbro is dominated by a singular in composition and in color. The metagabbro comprise massive rocks, highly weathered and jointed in most cases. Field observation indicates that they are intruded in metavolcaniclastic sequences and it is directly intruded by the tonalite-granodiorite rocks (Fig. 3, b).

II. Continental crust terrain. It is represented by (dokhan volcanic, gabbro, tonalite-granodiorite, monzogranite, alkali feldspar granite and dikes) as shown in Table 1.

II.1. Dokhan volcanic. It represents about 6% of exposed rock units in the mapped area Fig. 2; it is situated along the asphaltic road of Qena–Safaga near of Safaga city. Dokhan volcanic is characterized by imperial porphyry, medium to coarse – grained massive rock, reddish in color and highly jointed in NNE–SSW directions. It has high peaks one sets of joints one predominant trending NNE, casing the columnar like huge plugs. It is intruded directly by both of monzogranite and granitic porphyry with sharp contact between them, at the Qena–Safaga road, on the other hand, dokhan volcanic cut by basaltic dike with vertical shape (Fig. 3, c).

II.2. Gabbro. The gabbroic rock in the study area comprises as two types, layered and unlayered gabbro like purpose idea (Augland et al., 2011). The all two types of layered and unlayered gabbro are represented by small masses of moderately relief at the western side of Gable Um Taghir (Fig. 2). The unlayered gabbro has NW and NS trends and it is represented by low-moderate relief. It is characterized by medium to coarse – grained massive rocks, dark grayish to dark greenish color, not layered, highly fractured and deformed, sometimes smooth, generally one set of joints with predominant striking to 235° with vertical dipping to show well developed blocky structure, occasionally, shows spheroid shape (union shape) due to the weathering and exfoliation (Fig. 3, d), generally, unlayered gabbro intruded directly by granodiorite and monzo-

Table 1. Geochronology of the basement rocks in the study area.
Таблица 1. Геохронология пород фундамента в районе исследований.

Orogenic setting						Rock units	Age, Ma		Reference, Age
Late Cryogenian-Ediacaran magmatism	East African orogen EAO	Late-Post amalgamation	Late to post orogenic	Continental crust assemblage	Late to Post-orogenic	Dikes	650–542	Youngest	Johnson et al., 2011; Johnson, 2014
						Alkali feldspar granite			
						Monzogranite			
						Tonalite-granodiorite			
						Gabbro			
						Dokhan volcanic			
		Arc amalgamation	Early orogenic	Oceanic crust	Island arc assemblage	Metagabbro metavolcanoclastic	> 650	Oldest	

granite with sharp contact between granodiorite and gabbro, sometimes showing as big xenoliths. On the other hand, the layered gabbro is presented by small to medium masses at the middle of the study area (Fig. 2), which it is highly weathered, low land and highly altered. Occasionally, it is bearing ilmenite lenses in the bottom of the layered, this is related to magma rich of iron oxides. The layering type is trending strike 120/30 dipping SW, the ilmenite bands have the same direction of the layering. The bands are varying in thicknesses from few cm to about to 3m and more or less cross cut by quartz veins with SW trend.

II.3.1.Tonalite. It is restricted in south west of study area and represent reached about 13% of the early orogenic granitic rocks (Fig. 2), which it is characterized by grey in color and low hills, it is intruded directly by monzogranite and cross cut in metagabbro (Fig. 3, b), as well as, there is unconformity surface between the quaternary rocks (conglomerate) with tonalite, occasionally, conglomerate is characterized by boulders and rounded shape (Fig. 3, e).

II.3.2. Granodiorite. According to the field observations show that the granodiorite rocks are characterized by medium to coarse-grained with greyish in color, moderately relief and restricted in most of the study area (Fig. 2), it reached up to 87% of the granitoid constitution. There is sharp contact between the granodiorite and monzogranite (Abu Haweis granite), Fig. 3, f, on the other hand, monzogranite intruded in granodiorite (Gable Al Baroud), Fig. 3, g.

II.4.1. Monzogranite. It represents about 30% of study area, directly intruded in granodiorite (Fig. 3, g), as well as it's intruded by alkali feldspar granites granite by sharp contact, sometimes it represents as big xenoliths in alkali feldspar granite in Al Baroud and Abu Murat areas. It is white to pinkish in color, coarse to medium grained, massive rock and high relief in gable Abu Murat. It is characterized by highly jointed in two trends E–W and N–S, highly fractured due to the effect of a numerous faults trends, on the other hand the cavernous cavity and exfoliation are very common.

II.4.2. Alkali Feldspar Granites. It represents the latter type of the granitic magma in the study area. Generally, the alkali feldspar granite constitutes an elongated NS belt extending from Abu Haweis in the north to Wadi Um Taghir at the south (Fig. 2). It is represented by relatively high topographic relief up to ~890 m in Abu Hawies and represents about 5% of study area. It is characterized by massive, medium to coarse grained, pink to red color, and less jointed. Moreover, it is intruded through the granodiorite with sharp contact between them (Fig. 3, h).

II.5. Dikes and veins. In the area under investigated have many dikes and veins that differ in the composition and also in extruded time. They have different shapes and composition cutting all the older rocks are easily interpreted on the Landsat image, by their color, tone, contrast, linear shape and field relationships. Firstly, dikes range in thickness from 30 cm to about 15 m and extend to more than 15 km in length. They often comprise acidic dikes, intermediate (andesitic dike) and basic dikes (basaltic dike), Fig. 2. Acidic dikes are represented by granitic and rhyolite dikes as shown in Figs. 3, i, j. According to the field observations, andesitic dike cut alkali feldspar granite as shown in Fig. 3, k Finally, basaltic dikes cut many different rock units in the study area with deferent directions NE–SW,

E–W and NW–SE as shown in Fig. 3, l. Secondary, veins range in thickness from a few cm up to 7 m and extend to more than 5 km in length. They often comprise pegmatite, quartz veins and vein lets, as well as pegmatite vein cut in the granodiorite, it has up to 7 m thick as shown in Fig. 3, m, on the other hand, quartz veins and vein lets cut in the monzogranite as shown in Figs. 3, n, o.

Petrography

I. Island arc assemblage. The investigated of island arc assemblage consists of mostly the metavolcaniclastic and metagabbroic rocks. In the following sentences are the petrographical descriptions of them.

I.1. The metavolcaniclastic rocks. The metavolcaniclastic rocks are usually represented by actinolite-hornblende schist. **Actinolite-hornblende Schist**. It consist of plagioclase and quartz minerals. Iron oxides and apatite are the main accessory minerals; on the other hand actinolite, chlorite and epidote are the main secondary minerals. **Actinolite.** It is represented by euhedral-subhedral crystals up to 0.8 mm in length and 0.42 mm in width and ranging from 16.63% to 22.12% of the rock mineral constituents as show in Table 2. Actinolite has often pale to deep green color (Fig. 4, a). Mostly, actinolite crystals formed after alteration of the hornblende crystals as secondary minerals. **Hornblende.** It covers amount of rock composition ranging from 28.37% to 29.15 of the rock mineral constituents (Table 2). It is represented by subhedral to euhedral crystals up to 0.6 mm in length and 0.38 mm in width with green color strongly pleochroic to deep brown (Fig. 4, a). Sometimes they are deformed, altered to actinolite, epidote and chlorite minerals. **Plagioclase.** It is represented by subhedral crystals up to 0.32 mm in length and 0.2 mm in width, Carlsbad twining (Fig. 4, a) and forms about 14.09% to 17.08% of rock composition (Table 2). It is andesine in composition with anorthite content up to An_{43}. Sometimes, plagioclase is slightly altered to scerisite. **Quartz.** It covers amount of rock composition ranging from 14.06% to 13.64% (Table 2). It occurs as anhedral crystals and fine grains forming together with plagioclase the white bands of the schist (Fig. 4, a). **Chlorite.** It presents due to the alteration of actinolite and hornblende. Chlorite covers amount of rock composition ranging from 13.66 % to 15.4% (Fig. 4A) while epidote occurs as euhedral prismatic crystals accounting within the hornblende ones. Iron oxide: It is represented by dark black irregular grains, associating with hornblende up to 3.38% of rock composition (Table 2). **Apatite**. It is present as fine subhedral colorless crystals associating with the hornblende forming an amount up to 1.2% of rock composition (Table 2).

I.2. Metagabbro. They are characterized by less deformed of greenish black massive rocks, in general showing porphyritic texture as a common texture of the investigated metagabbro. According to QAP diagram of Streckeisen (1976). The studied samples are fall in intermediate metagabbro in composition. The modal composition of the investigated metagabbroic rocks are given in Fig. 5, a and Table 3. The metagabbro is mainly consists of plagioclase, augite, hornblende, quartz and biotite in addition to iron oxide and apatite as accessory minerals, while chlorite and epidote are present as mineral assemblage secondary minerals. **Plagioclase**. This mineral is the most representative of all mineral constituents of the investigated metagabbro that is varying from 52.6 % to 55.6% of the all rock
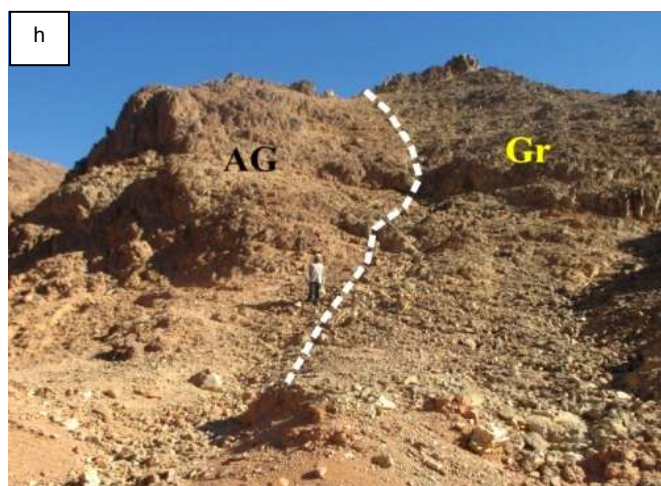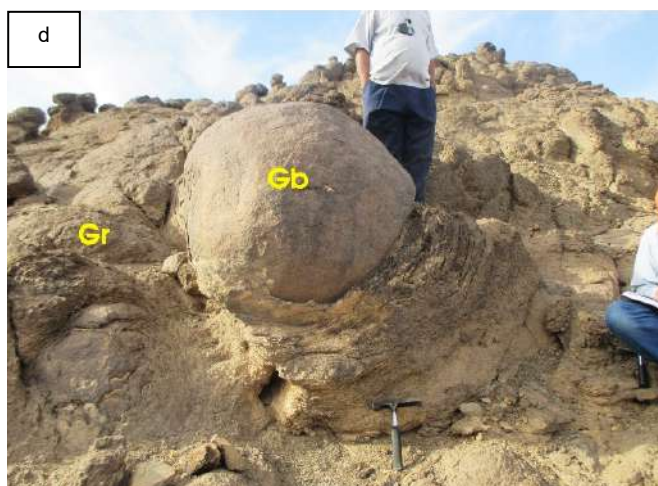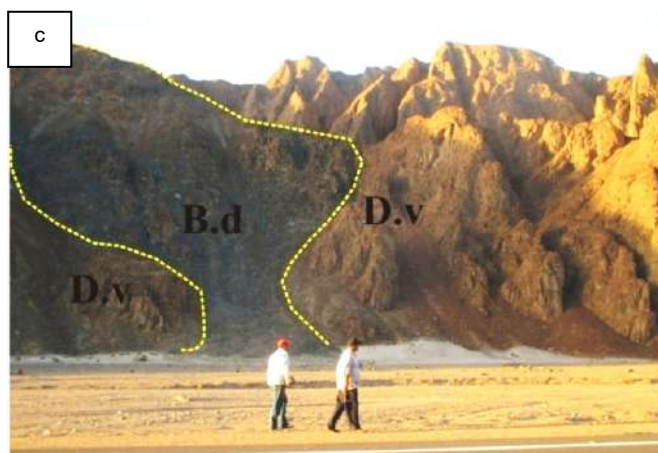
Figure 3. Photographs showing. a – well-developed schistosity of the metavolcanoclastic rocks; b – metagabbro (M.g) intruded by the tonalite-granodiorite (Gr) at Gable Abu Furad; c – basaltic dike (B.d) cutting in dokhan volcanic (D.v) at Qena–Safaga road; d – spheroidal shape of gabbro (Gb) as xenoliths in granodiorite (Gr) at Wadi Al-Baroud; e – unconformity surface between sedimentary rocks (Cg) and tonalitic rocks (G) at Wadi Um Taghi; f – sharp contact between granodiorite (Gr) and monzogranite (Mz) at Gable Abu Hawies; g – granodiorite (Gr) intruded directly by monzogranite (Mz) at Gable Al Baroud; h – sharp contact between granodiorite (Gr) and alkali feldspar granite (AG) at Wadi Um Taghir; i – granitic dike (Gr.d) cutting in granodiorite (Gr) at Wadi Al Baroud; j – rhyolite dike (R.d) cutting in monzogranite (Mz) at Wadi Um Taghir; k – andesitic dike (An.d) cutting in alkali feldspar granite (Ak.g) with NE–SW directions at at Wadi Al Baroud; l – basaltic dike (B.d) cutting in gabbro (Gb) EW trending at Wadi Al-Baroud; m – pegmatite vein cutting in the granodiorite (Gr) at Wadi Al Baroud; n – Quartz vein (Q.v) cutting in the monzogranite (Mz) with direction E–W at Abu Hawies; o – quartz vein lets (Q.v) cutting in the monzogranite (Mz) with directions E–W and N–S at Abu Hawies.

Рисунок 3. Фотографии. а – хорошо развитая сланцеватость метавулканокластических пород; b – метагаббро (M.g), интрудируемые тоналитом-гранодиоритом (Gr) в Гейбл Абу-Фураде; с – базальтовая дайка (B.d) в вулканитах доханской свиты (D.v) в направлении дороги Кена–Сафага; d – сфероидальная форма габбро (Gb) в виде ксенолитов в гранодиорите (Gr) в Вади-эль-Баруде; е – поверхность несоответствия между осадочными породами (Cg) и тоналитовыми породами (G) в Вади Ум Тагире; f – резкий контакт между гранодиоритом (Gr) и монцогранитом (Mz) в Гейбл Абу Хависе; g – гранодиорит (Gr), непосредственно интрудируемый монцогранитом (Mz) в Гейбл-эль-Баруде; h – резкий контакт между гранодиоритом (Gr) и щелочно-полевошпатовым гранитом (AG) в Вади Ум Тагире; i – гранитная дайка (Gr.d) в гранодиорите (Gr) в Вади Аль Баруде; j – риолитовая дайка (R.d) в монцограните (Mz) в Вади Ум Тагире; k – андезитовая дайка (An.d) в щелочно-полевошпатовом граните (Ak.g) с направлениями NE-SW в Вади-эль-Баруде; l – базальтовая дайка (B.d) в габбро (Gb) в направлении EW в Вади-эль-Баруде; m – пегматитовая жила в гранодиорите (Gr) в Вади-эль-Баруде; n – кварцевая жила (Q.v) в монцограните (Mz) с направлением E-W в Абу-Хависе; о – кварцевая жила в (Q.v) монцограните (Mz) с направлениями E-W и N-S в Абу-Хависе.

composition as showing in Table. 3, it is occurred as medium to coarse grains, which it is up to 1.8 mm in length and 1 mm in width (Fig. 4, b). Generally the composition of plagioclase is ranging from labradorite (An_{62}) to bytownite (An_{79}). It is partly to totally deformed or altered to scerisite mineral. **Augite.** It is represented by subhedral and anhedral crystals of pale yellow color pleochroing to dark yellow color (Fig. 4, b) and forms an amount up to 13% of rock composition as showing in (Table 3). It is often colorless under ordinary light with two set of cleavage. On other hand, augite is altered to chlorite and epidote. **Hornblende.** It is represented by subhedral to anhedral crystals of medium grained, it is characterized by brownish in color, sometimes showing destroyed**,** which it is up to 0.78 mm in length and 0.44 mm in width and varying in volume from 14.94% to 16.6% of rock composition. It has two sites of cleavage (Fig. 4, b), sometimes hornblende altered to chlorite. **Quartz.** It is represented by anhedral crystals up to 0.38 mm in length and 0.18 mm in width. As well as, the crystals are filing the interstitial spaces of most mineral constituents as shown in Fig. 4, b. It is manly ranging from 3.049% to 4.59% of the rock composition (Table 3). **Biotite.** It is represented by subhedral crystals up to 3.4% of rock composition (Table 3), it is characterized by pale yellowish crystals and pleochroing often to brown color. Sometimes biotite is altered to chlorite and epidote. **Chlorite and epidote.** They are represented by green to pale green crystals. It occurs as secondary mineral mainly, occur due to alteration of the mafic minerals, chlorite covers about 5.25–6.25 % of rock composition, while epidote covers about 1.7–1.88% of rock composition (Table 3). **Iron oxides**. They are represented by dark grains associating within the mineral constituents. **Apatite.** It is represented by fine euhedral crystals scattering within the hornblende**.**

II.1. Dokhan volcanic. It exhibits often porphyritic texture. According to QAP classification diagram of volcanic rocks of Streckeisen (1976), it has been andesite in composition (Fig. 5, b). It is composed essentially of plagioclase, hornblende and biotite, with few amounts of quartz and alkali felspar. Iron oxides are the accessory minerals. Sometimes it is character-

ized by porphyritic texture (Fig. 4, c). **Plagioclase.** It occurs as andesine composition (An_{30}–An_{40}), covering an area up to 59% of main rock constituents. It is represented by euhedral to subhedral crystals, up to 1.6 mm in length and 0.8 mm in width, sceriste. **Quartz**. It covers an area up to 11% of rock constituents, occurs as fine-grained anhedral subordinate crystals and distributed among other mineral constituents. **Hornblende.** It is represented by subhedral to anhedral crystals, covers an area ranging from 11% to 13% of mineral compositions of rock. It is green in color pleochroing from green (=X) to pale brown (=Y) and brown (=Z), it is partly or completely altered to chlorite. **Biotite.** It occurs as flaky crystals, up to 0.4 mm in length and 0.2 mm in width. Biotite covers an area ranging from 10% to 14% of rock compositions, sometimes, it is altered to chlorite (Fig. 4, c). **Alkali feldspar.** It occurs as fine to medium grained, up to 0.04 mm in length and 0.02 mm in width. It covers an area up to 5% of rock compositions, sometimes; it is represented by microcline and orthoclase crystals associated with other minerals of rock. **Iron oxides.** They are represented by deep black grains scattering over the rock mineral constituents and disseminated within the different minerals. **II.2. Gabbroic rocks.** According to their modal composition as shown in Table 5 the studied rock samples are plotted on plagioclase, pyroxene and hornblende IUGS diagram, which it is given by Le Maitre (2002), the gabbroic rocks are classified into pyroxene hornblende gabbro and leucogabbro (Fig. 5, c).

II.2.A. Pyroxene Hornblende Gabbro. It is characterized by medium to very coarse-grained rock, showing often subordinate ophitic and sub ophitic textures (Fig. 4, d). It consists mainly of plagioclase, pyroxenes and hornblende. Chlorite and actinolite present as secondary minerals. The accessory mineral is iron oxides. **Plagioclase.** It is represented by tabular-euhedral to subhedral crystals, up to 3.2 mm in length and 1.6 mm in width, it has labradorite composition with anorthite content ranging from (An_{57} to An_{67}), covers about 60% of the rock composition (Table 5). The plagioclase often shows albite-Carlsbad twinnings, as well as it shows weak zonation and intergrowth with pyroxene to show well developed ophitic and

Table 2. Modal composition of metavolcaniclastic sequences.
Таблица 2. Модальный состав метавулканических последовательностей.

Serial number	Sample number	Actinolite	Horn-blende	Plagio-clase	Quartz	Iron oxide	Epidote	Apatite	Chlorite	Total
1	73	13.63	18.37	19.08	27.2	2.29	1.73	1.04	16.66	100
2	72	22.12	29.15	14.09	13.64	3.38	1.02	1.2	15.4	100
3	72b	14.63	17.37	20.08	25.22	2.27	1.73	1.04	17.66	100
4	71	22.12	29.15	14.09	13.64	3.38	1.02	1.2	15.4	100
	Av	19.4	28.8	15.57	16.4	2.8	1.37	1.12	14.5	100

Table 3. Modal composition of metagabbro.
Таблица 3. Модальнй состав метагаббро.

Serial number	Sample number	Pla-gioclase	Augite	Horn-blende	Quartz	Chlorite	Epidote	Iron oxide	Biotite	Apatite	Total
1	74a	55.6	11	14.94	4.59	6.25	1.76	4.02	2	0.4	100
2	70	53.4	12	16.6	3.04	5.25	1.88	5.57	1.6	0.66	100
3	70b	52.6	13	15.8	4.19	5.65	1.7	4.12	3.4	1	100
	Av.	53.86	12	15.78	3.94	5.71	1.78	4.54	2.3	0.66	100

Table 4. Modal composition of the andesitic rocks.
Таблица 4. Модальный состав андезитовых пород.

Rock name	Sample number	Quartz	Pla-gioclase	Alkali felspar	Pyrox-ene	Horn-blende	Biotite	Musco-vite	Iron oxide	Chlorite	Total
Andesite	57	11	58	3	–	13	10	–	3	2	100
	61A	9	56	4	–	11	14	–	3.6	2.4	100
	63	8	59	5	–	12	13	–	2	1	100
	Av.	9.3	57.7	4	–	12	12.3	–	2.85	1.8	100

Table 5. Modal composition of the gabbroic rocks.
Таблица 5. Модальный состав габброидов.

Sample number		Plagioclase	Pyroxene		Olivine	Horn-blende	Chlorite	Actino-lite	Iron oxide	Total
			Augite	Hypersthene						
Leucogabbro	6	65	25	3.8	3	–	1	1	1.2	100
	38A	67	23.6	4.4	2.2	–	1	0.8	1	100
	39	69	25	2.6	2.3	–	0.2	0.4	0.5	100
	40	68	24	2.3	2	–	0.4	1	1.7	100
Average value		67.25	24.4	3.3	2.4	–	0.7	0.8	1.1	100
Pyroxene-Horn-blende Gabbro	55	60	18	4	–	13	2.6	1	1.4	100

sub-ophitic textures (Fig. 4, d). **Pyroxenes.** It is represented by augite and little amount of hypersthenes, covers about 22% of the rock composition. **Augite.** It is represented by euhedral to subhedral crystals, up to 1.76 mm in length and 1.2 mm in width. Sometimes, it is partly altered to chlorite. **Hypersthene.** It is represented by anhedral crystals, covers about 4 % of the rock composition. It is characterized by pale to green pleochroism and parallel extinction. Occasionally, it fills the interstitial spaces between the mineral constituents sometimes as a rim (Fig. 4, e). **Hornblende.** It is represented by euhedral to subhedral crystals, up to 1.6 mm in length and 0.7 mm in width. It covers about 13% of the rock composition. Often, it is characterized by brown in color with strong pleochroism from green to brown generally; it shows two sets of cleavage (60–120) and high relief, sometimes it is altered to chlorite and actinolite. **Chlorite.** It is generally represented by subhedral crystals, with green to pale green colored as secondary mineral, associating with pyroxene. **Iron oxides**. They are represented by cubic black crystals, often occur as fine grains scattering over the rock mineral constituents, disseminated within the different minerals.

II.2.B. Leucogabbro. This type consists mainly of plagioclase, pyroxenes and olivine. On the other hand accessory minerals are iron oxides and apatite. While actinolite and chlorite occur as secondary minerals. Sometimes, it exhibits subordinate ophitic to sub-ophitic textures (Fig. 4, f). **Plagioclase.** It is represented by euhedral to subhedral crystals up to 1.8 mm to 2.2 mm in length and 1 mm to 1.1mm in width. It covers ranging from 65% to 69% by volume of the rock constituents; it has labradorite to bytownite compositions with anorthite content (An_{68}–An_{79}). Occasionally, it is characterized by albite and Carlsbad twinnings. Sometimes, it shows weak zonation and occurs within pyroxene showing well develop ophitic and sub-ophitic textures (Fig. 4, f). **Pyroxenes.** There are two main types, clinopyroxene (augite) and orthopyroxene (hypersthene), they cover about from 27.6% to 28.8% of the

rock composition. Augite is more present than hypersthene. It occurs as subhedral to anhedral crystals, up to 2 mm in length and 1.4 mm in width. It covers about from 23.6 % to 26 % of the rock composition. Augite is characterized by pale green pleochroism. On the other hand, orthopyroxene is mainly hypersthenes covers up to 4.4% of the rock composition, which occurs as subhedral crystals filling the interstitial spaces between the mineral constituents. **Olivine.** It occupies about from 2.2% to 3% of the rock composition. Olvine is represented by subhedral crystals up to 1.6 mm in length and 0.6 mm in width. Sometimes, it is fractured and altered. The fractures are filed by opaque minerals. It is often rimmed by pyroxene (hypersthene) and actinolite (Fig. 4, f). **Iron oxides.** They occur as medium to course deep black grains scattering over the rock mineral constituents and disseminated within the different minerals. **Actinolite.** It occurs as secondary minerals, according to altered primary minerals along the margins of pyroxene and olivine. **Chlorite.** It is represented by subhedral crystals with pale green colored as secondary mineral after pyroxene.

II.3. Early orogenic granites. They comprise essentially the tonalite and granodiorite, according to their modal composition (Table 6), plotted on QAP diagram of Streckeisen (1976), Fig. 5, d.

II.3.1. Tonalite. It is represented by plagioclase, quartz, biotite and hornblende, while sphene, zircon and iron oxide occur as accessory minerals, on the other hand chlorite occurs as secondary mineral. **Plagioclase.** It is represented by andesine in composition (An_{22-37}) ranging from 49.6% to 52.4% of the rock mineral constituents. It occurs as euhedral and subhedral prismatic crystals up to 0.23 mm in width and 0.8 mm in length, characterized by Carlsbad twinning (Fig. 4, g). **Quartz.** It covers area ranging from 28% to 32.5% of the rock mineral constituents. Occasionally, it is occurred as anhedral crystals with different sizes, displaying often wavy extinction (Fig. 4, h). **Biotite.** It covers an area up to 7% of the rock mineral constituents. It occurs as euhedral to subhedral crystals up to 0.4

Table 6. Modal composition of early orogenic granites.
Таблица 6. Модальный состав ранних орогенных гранитов.

Sample number	Quartz	Pla-gioclase	Alkali felspar	Biotite	Hornblende	Sphene	Chlorite	Iron oxide	Total
				Tonalite					
42	31.9	51	3	6	4	–	2	2.1	100
65	30.5	50.6	4	5,5	6	–	1.5	1.9	100
69A	25	50	1.6	7	10	1	2	3.4	100
79	32.5	49.6	4	5	6	–	1	1.9	100
Av.	30	50.3	3.15	6	6.5	0.25	1.6	2.3	100
				Granodiorite					
21	31	47	14	5	1	–	2	1	100
23	35	45	15	1	1.6	0.4	0.5	1.5	100
26A	28	48	17	4	1	–	1	1	100
28A	27	49	16	4	0.9	–	2	1.1	100
31A	30	44	18	5	1	–	1	1	100
46	31	42	19	4	1.6	0.3	0.6	1.5	100
66	26	50	16	5	–	–	2	1	100
75	32	42	17	6	08	–	2	1.2	100
76	34	46	15	1	1.6	0.4	0.5	1.5	100
Av.	30.4	45.9	16.3	4	1	0.12	1.3	1.16	100

Table 7. Modal composition of the late to post orogenic granites.
Таблица 7. Модальный состав поздних посторогенных гранитов.

Sample number	Quartz	Plagioclase	Monzo-granite	Ortho-clase	Perthite	Biotite	Musco-vite	Chlorite	Actinolite	Total
			Monzogranite							
1	28	33	20	6	9	1	2	–	1	100
4	30	25	25	5	10	1	1	1.5	1.5	100
11	27	30	22	6	11	2	–	1	1	100
13	28	32	23	4	9	3	–	0.5	1.5	100
16	25	26	30	3	9	4	1	1	1	100
28B	23	30	32	3	9	1	1	–	1	100
33A	25	32	29	6	7	1.5	–	–	0.5	100
35	27	33	27	3	8	1	–	–	1	100
52A	32	29	26	3	6	1	0.5	0.5	1.5	100
54	30	26	24	5	10	1	1	1.5	1.5	100
61B	30	31	23	2	9	3	–	0.5	1.5	100
74B	28	32	26	4	8	1	–	–	1	100
78	29	27	27	5	8	1	–	1	2	100
Av.	27.8	29.7	25.7	4.2	8.7	1.7	0.5	0.6	1.12	100
			Alkali feldspar granite							
14A	31	6	7	1	53	–	1	–	1	100
19A	26	2	5	–	60	–	5	–	2	100
33B	39	1	8	–	49	–	2	–	1	100
36	30	5	10	1	50	–	2.5	–	1.5	100
52B	40	3	7	–	48	–	1.5	–	0.5	100
Av.	33.2	3.4	7.4	0.4	52	–	2.4	–	1.2	100

Table 8. Modal composition of the investigated dikes.
Таблица 8. Модальный состав исследованных даек.

Rock name	Serial number	Quartz	Pla-gioclase	Alkali fel-spar	Horn-blende	Pyrox-ene	Bio-tite	Musco-vite	Iron oxide	Chlorite	Total
Granitic dikes	9	35	25	33	–	–	1	3	3	–	
	50	30	37	23	2	–	3	1	3	1	100
	26C	34	24	36	–	–	–	3	3	–	100
	Av.	33	28.7	30.6	0.67	–	1.3	2.33	3	0.3	100
Andesitic dike	19B	8	57	–	17	–	11	–	5	2	100
	19C	9	60	–	15	–	10	–	4	2	100
	19D	7	58	–	18	–	12	–	4	1	100
	Av.	8	58.3	–	16.7	–	11	–	4.33	1.7	100
Rhyolitic dike	43A	32	25	33	–	–	3	4	3	–	100
	43B	33	26	32	–	–	2	3	4	–	100
	43C	34	23	34	–	–	4	2	3	–	100
	Av.	33	24.7	33	–	–	3	3	3.3	–	100
Basaltic dike	14B	1	62	–	–	31	–	–	2	4	100
	33c	2	66	–	–	28	–		1	3	100
	31B	1	66	–	–	29	–	–	3	1	100
	Av.	1.7	64.7	–	–	29.3	–	–	2	2.7	100

mm in length and 0.2 mm in width of pale brown color, strong pleochroic to deep brown color (Fig. 4, g). **Hornblende.** It occurs as subhedral and anhedral crystals associated with quartz and plagioclase crystals, in filtered often by quartz crystals and covers up to 6% of the rock mineral constituents. It is characterized by two sets of cleavage and yellowish green color (Fig. 4, h). **Sphene.** It is represented by variable contents, covers an area up to 1% of the rock mineral constituents as prismatic crystals up to 0.1 mm in length and 0.08 mm in width . **Iron oxides**. They are represented by deep black grains scattered over the rock mineral constituents and disseminated within the different minerals. **Chlorite.** It occurs as secondary mineral after biotite in most cases or hornblende as green bands often parallel with the cleavage of biotite crystals.

II.3.2. Granodiorite. It is composed mainly of plagioclase, quartz and orthoclase as essential minerals, while apatite, biotite and iron oxide represent the accessory minerals; on the other hand chlorite occurs as secondary mineral. **Plagioclase.** It is mainly ranging in composition from oligoclase ($An_{16–26}$) and andesine ($An_{32–36}$) in composition. It covers an area up to 50 % of the main mineral of the rock constituents, represented by euhedral and subhedral crystals up to 1.2 mm in length and 0.7 mm in width, showing Carlsbad twinning's of plagioclase (Fig. 4, i). **Quartz.** It covers an area up to 36% of the main rock constituents, represented by anhedral crystals, sometimes, filling the interstitial spaces of the mineral constituents, characterized by showing wavy extension, as well as fine grained crystals associated with other minerals such as plagioclase and biotite (Fig. 4, i). **Orthoclase.** It covers area ranging from 14% to 19% of the rock composition, represented by medium to coarse subhedral crystals up to 1 mm in length and 0.6 mm in width (Fig. 4, j). **Biotite.** It occurs as flaky crystals, covers an area up to 6% of the main rock constituents. It is characterized by one set of cleavage, enclosing some iron oxide. It is observed also, as fine biotite crystals enclosed by the plagioclase (Fig. 4,

i), sometimes, some crystal of biotite partly altered to chlorite. **Hornblende.** It is represented by euhedral crystals up to 1 mm in length with 0.6 in width, covering an area up to 1.6% of rock composition and characterized by strongly pleochroic green (=X) to deep green (=Y) and brown (=Z) colors. **Sphene.** It is represented by subhedral crystals up to 0.09 mm in length and 0.04 mm in width. It covers an area ranging from 0.1% to 0.4% of the main rock constituents, enclosed by plagioclase crystals. **Iron oxide.** It is represented by deep black grain scattering over the rock mineral constituents and disseminated within the different minerals. It covers an area up to 1.5 % of the rock composition (Fig. 4, i). **Chlorite.** It occurs as secondary minerals after alteration process of biotite and hornblende crystals.

II.4. Late to post orogenic granites. According to modal composition of the late to post orogenic granites given in Table 7 and plotting on QAP diagram of Streckeisen (1976), they have composition of monzogranite and alkali feldspar granite (Fig. 5, e).

II.4.1. Monzogranite. It is composed mainly of alkali feldspar, plagioclase, quartz, muscovite and biotite as essential minerals, chlorite as secondary minerals, iron oxides, apatite and sphene as accessory minerals. **Alkali feldspars.** They cover about 43% of the rock composition as shown in Table 7. They are represented often by microcline and orthoclase as well as microcline perthite determined as vein and flaky types (Fig. 4, k). The microcline crystal has often cross-hatching twinning, covering an average about 30% of rock composition (Table 7). It occurs as subhedral and platy crystals up to 1.6 mm in length and 0.9 mm in width. On the other hand, orthoclase crystal occurs as euhedral to subhedral crystals up to 1.2 mm in length and 0.65 mm in width, enclosing some sphene fine-grain crystals. It covers about 4.25% of rock composition. The flaky microcline perthite is represented by many of flaky albite crystals distributed over the microcline crystal, covering about 8.6% of mineral constituents of rock. **Plagioclase**. It
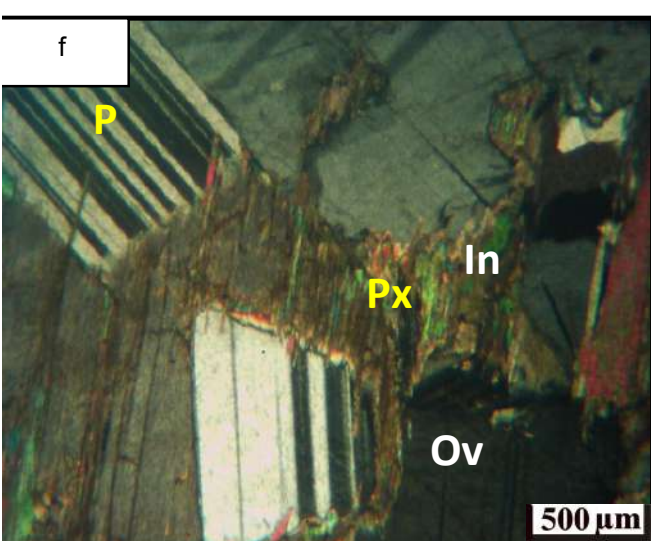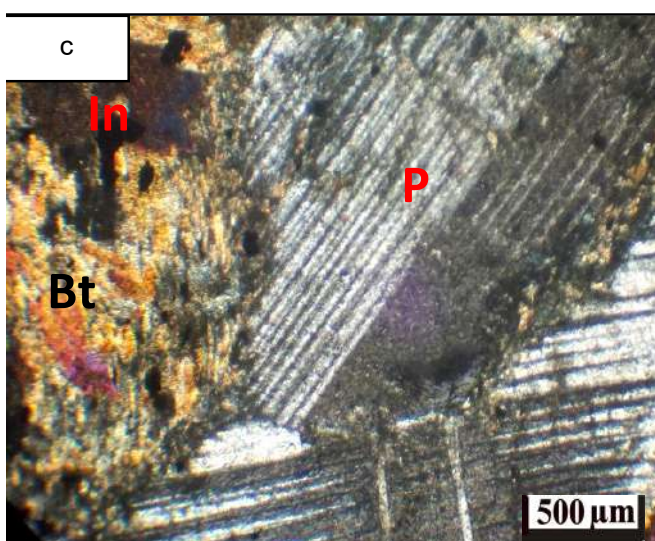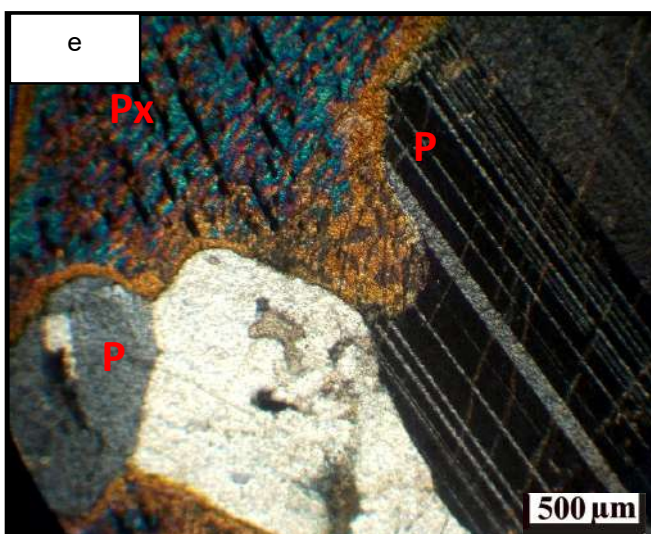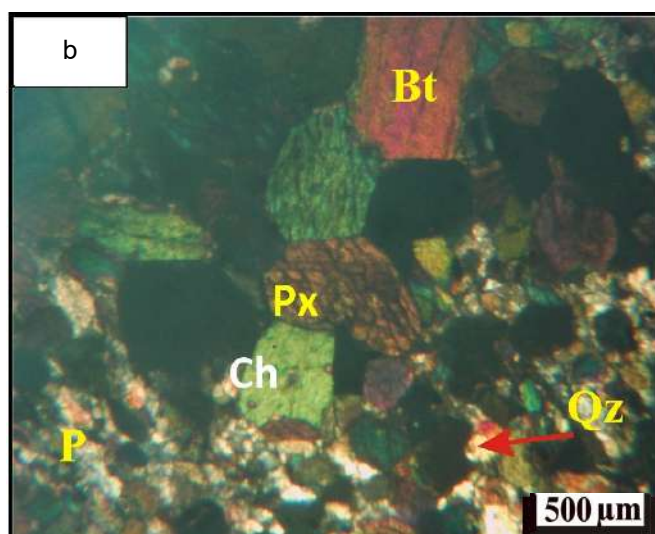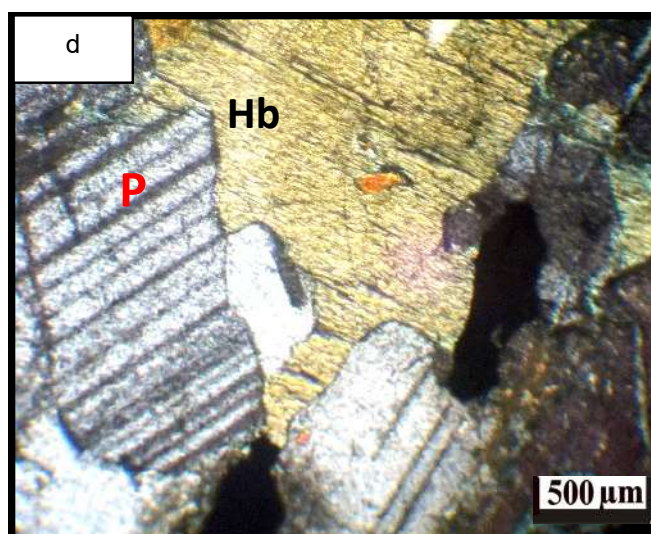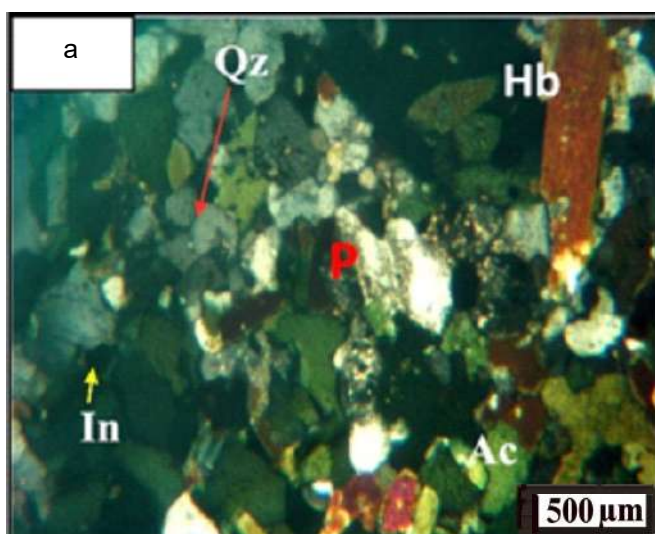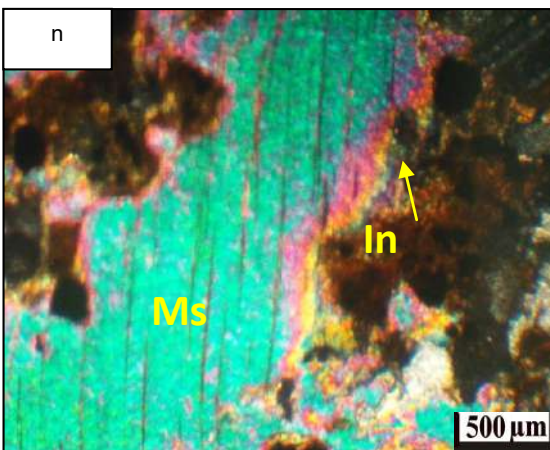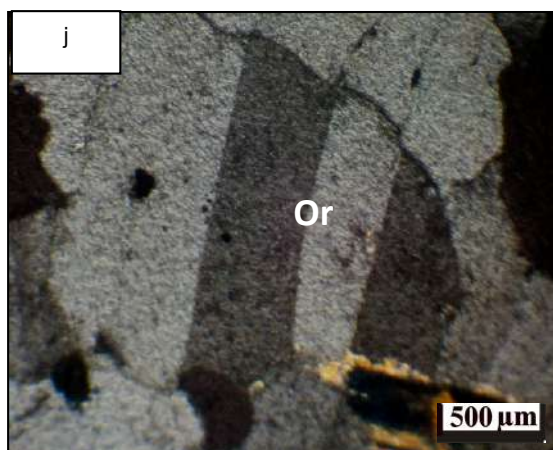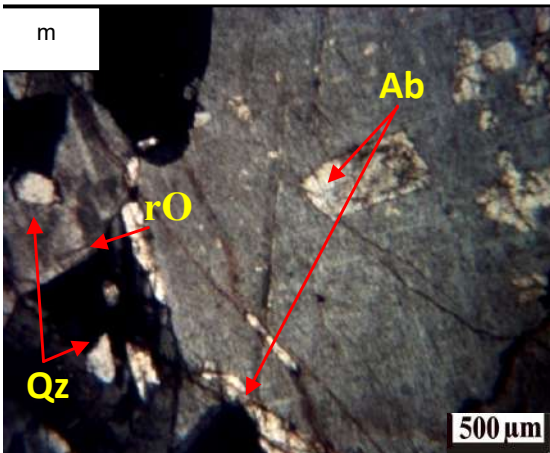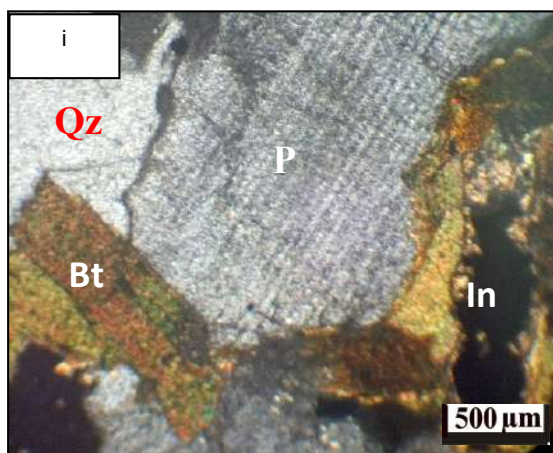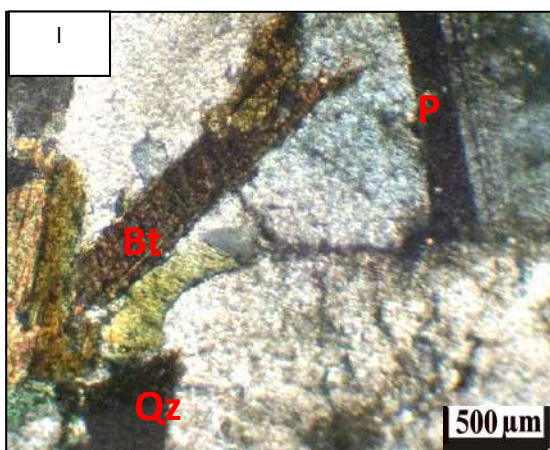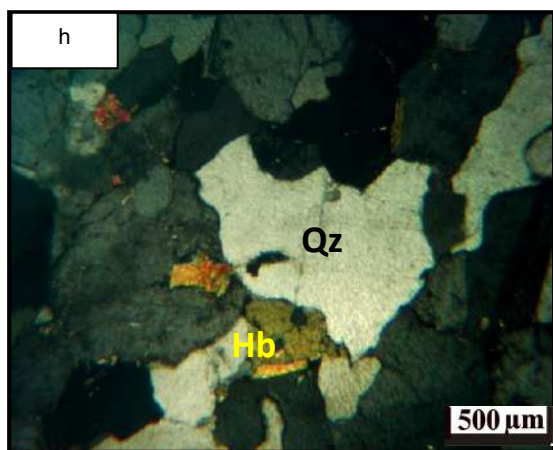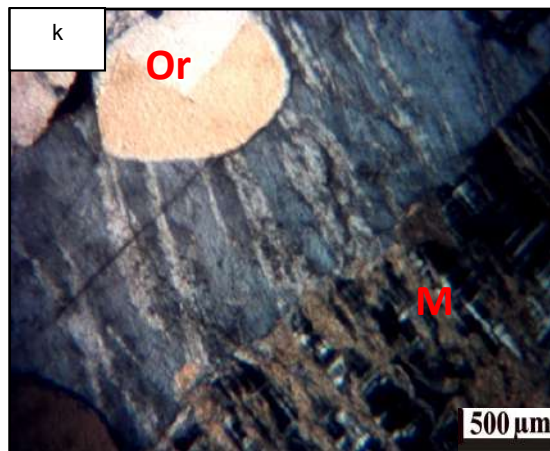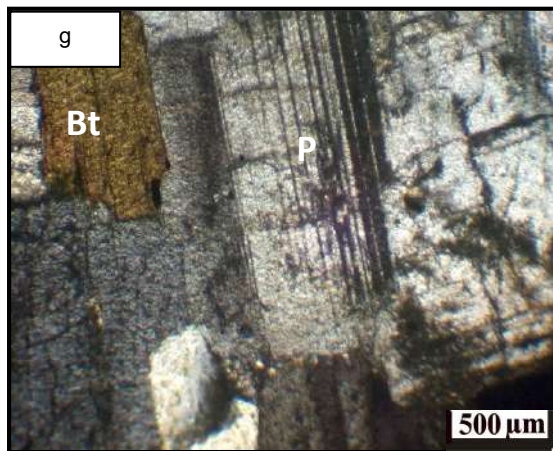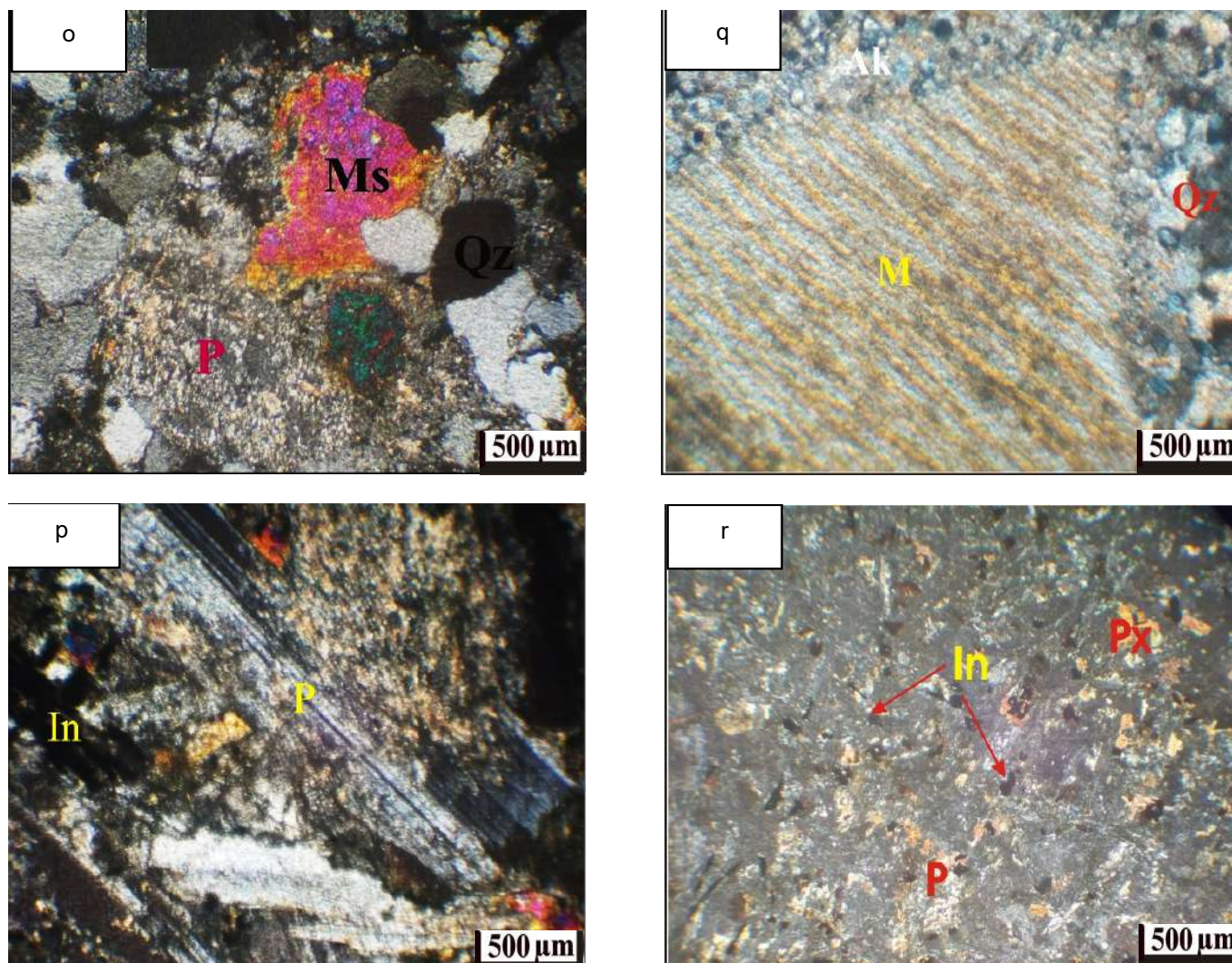
Figure 4. Photomicrographs showing actinolite mineral (Ac) within some fine grains of plagioclase (P), quartz (Qz) and hornblende (Hb) in actinolite-hornblende schist (a); plagioclase (P) within large corroded grain of augite (Px), chlorite (Ch) and biotite (Bt) in the metagabbro (b); phenocrystal of plagioclase (P) surrounded by fine grains groundmass to show porphyritic texture in andesite (c); subhedral hornblende (Hb) enclosing with albite and Carlsbad twins of plagioclase (P) in pyroxene hornblende gabbro (d); augite grain (Px) inclosing grains of plagioclase (P) to show ophitic texture (e); olivine (Ov) growing with plagioclase (P) in leucogabbro (f); subhedral crystals of biotite (Bt) associated with Carlsbad crystal of plagioclase (P) in tonalite (g); anhedral crystal of quartz (Qz) associated with hornblende (Hb) in tonalite (h); albite twin plagioclase (P) associated with quartz grains (Qz) and flakey of biotite (Bt) in granodiorite (i); subhedral crystal of orthoclase (Or) in granodiorite (j); flaky of strain microcline perthite (M) associated with subhedral crystal of orthoclase (Or) in monzogranite (k); flaky of biotite (Bt) associated with Carlsbad twin of plagioclase (P) in monzogranite (l); albite of plagioclase (Ab) enclosed in microcline of vein perthite to show rapakivi texture in alkali feldspar granite (m); big crystal of muscovite (Ms) with minor crystals of iron oxides (In) scattered in alkali feldspar granite (n); subhedral crystal of plagioclase (P) associated with alkali feldspar, quartz crystal (Qz) and muscovite (Ms) in the granitic dike (o); euhedral crystal of plagioclase (P) partly altered to serisite associated with biotite partly altered to chlorite (Bt), hornblende crystal and fine grains of iron oxides (In) in the andesite dikes (p); microcline vein perthite (M) surrounded by fine grains of quartz (Qz) to show porphyritic texture in the rhyolite dike (q); fine-grained plagioclase crystals (P) associated with pyroxene crystals (Px) and fine grained of iron oxides (In) in the basalt dikes (r). (C.N.).

Рисунок 4. Фотографии шлифов, показывающие актинолит (Ac) в агрегате мелких зернах плагиоклаза (P), кварца (Qz) роговой обманки (Hb) в сланце актинолитроговообманковом сланце (a); плагиоклаз (P) в крупном корродированном зерне авгита (Px), хлоритом (Ch) и биотитом (Bt) в метагаббро (b); фенокристалл плагиоклаза (P), окруженный мелкозернистой основной массой, демонстрирующий порфиритовую текстуру в андезите (c); субгедральная роговая обманка (Hb), окруженная альбитом и карлсбадскими двойниками плагиоклаза (P) в пироксен-роговообманковом габбро (d); зерно авгита (Px), содержащее зерна плагиоклаза (P), демонстрирующее офитовую текстуру (e); оливин (Ov), срастающийся с плагиоклазом (P) в лейкогаббро (f); субгедральные кристаллы биотита (Bt), в ассоциации с карлсбадским кристаллом плагиоклаза (P) в тоналите (г); идиоморфный кристалл кварца (Qz), в ассоциации с роговой обманкой (Hb) в тоналите (h); альбитовый двойник плагиоклаза (P), в ассоциации с зернами кварца (Qz) и лейстами биотита (Bt) в гранодиорите (i); субгедральный кристалл ортоклаза (Or) в гранодиорите (j); деформированный микроклиновой пертит (M), в ассоциации с субгедральным кристаллом ортоклаза (Or) в монцограните (k); лейст биотита (Bt), в ассоциации с карлсбадским двойником плагиоклаза (P) в монцограните (l); альбит (Ab), заключенный в жильный микроклин, демонстрирующий структуру рапакиви в щелочном полевом шпате (m); большой кристалл мусковита (Ms) с мелкими кристаллами оксидов железа (In), рассеянных в щелочно-полевошпатовом граните (n); субгедральный кристалл плагиоклаза (P), в ассоциации с щелочно-полевошпатовым гранитом, кварцем (Qz) и мусковитом (Ms) в гранитной дайке (o); идиоморфный кристалл плагиоклаза (P), частично амещенный серизитом в ассоциации с биотитом, частично амещенный хлоритом (Bt), а также кристаллы роговой обманки и мелкие зерна оксидов железа (In) в андезитовых дайках (p); жилы микроклина-пертита (M), окруженный мелкими зернами кварца (Qz), демонстрирующие порфиритовую текстуру в риолитовой дайке (q); мелкозернистые кристаллы плагиоклаза (P), связанные с кристаллами пироксена (Px) и мелкозернистые оксиды железа (In) в дайках базальта (r). (C.N.).

occurs as oligoclase crystals in composition, which it is varying from (An_{13}) to (An_{21}), covering about 29.5% of the rock mineral constituents. It is represented by euhedral to subhedral crystals up to 1.6 mm in length and 0.8 mm in width exhibiting often Carlsbad twinning (Fig. 4, l), while primary zonation is less common, some crystals enclose some opaque minerals such as iron oxides and also infiltrated by quartz and biotite to form subordinate poikilitic texture. **Quartz**. It occurs as anhedral crystals up to 0.85 mm in length and 0.44 mm in width, covering about 27.8% of the rock composition as interstitial components, as well as minor minute's crystals distributed over all the mineral composition as seen in **Muscovite**. It covers an area up to 0.5% of the rock constituents as show in Table 7. It is represented by flaky crystals up to1 mm in length and 0.6 mm in width, probably developed during alteration of rock by the late magmatic reaction, characterized often by high interference color and reacted rims. Sometimes, it is altered to chlorite crystals (Fig. 4, l). **Biotite**. It is represented by euhedral to subhedral crystals, covering about 1.5% of the main rock constituents, characterized by one set of cleavage, associated with the plagioclase, quartz crystals and partly altered to chlorite (Fig. 4, l). **Chlorite.** It occurs as secondary mineral, after alteration of biotite and muscovite, with pale green color in most cases (Fig. 4, l). **Iron oxides.** They are represented by deep black grains scattered over the rock mineral constituents and disseminated within the different minerals. They occur with considerable value up to 1 % of the rock composition. **Sphene**. It is represented by fine grain crystal, covering about 0.2% of the main rock constituents and associated with different mineral compositions of rock. **Apatite**. It occurs as euhedral prismatic crystal enclosed essentially in the alkali feldspar crystals.

II.4.2. Alkali feldspar granite. It consists mainly of alkali-feldspars, quartz, plagioclase and muscovite. Biotite is less common. On the other hand, sphene and iron oxides are the main accessory minerals. While chlorite is the main secondary mineral. **Alkali feldspars.** They cover an amount of 59.8 % of the rock composition as showing in (Table 7). They consist essentially of microcline, microcline perthite and orthoclase (Fig. 4, m). Microcline covers about 7.4% of the rock composition. It is represented by subhedral or rectangular crystals up to 1.8 mm in length and 1.2 mm in width. It shows clear cross-hatching twinning. Sometimes, it is partly altered to kaolinite, as well as it encloses plagioclase and quartz crystals. On the other hand, microcline perthite is covers about 46% of the rock constituents. It occurs as subhedral to anhedral platy crystals, reaching up to 2.4 mm in length and 1.6 mm in width. Occasionally, microcline perthite mantled by small crystal of plagioclase to show rapakivi texture (Fig. 4, m). Orthoclase is the less common constitution, which is covers about 6.4% of rock composition. It is represented by subhedral to anhedral crystals up to 1.2 mm in length and 0.8 mm in width. The perthites are usually occurring as vein and patchy perthites. **Quartz.** It covers about 33.2 % of rock constituents (Table 7). It is represented by subhedral to anhedral crystals of various shape and size (Fig. 4, m), it characterized by wavy exctential, sometimes it fills the interstitial spaces of the rock composition. It reaches about 1.4 mm in length and 0.9 mm in width. **Plagioclase.** It occurs as euhedral to subhedral prismatic crystals. It reaches up to 2 mm in length and 1.2 mm in width, with anorthite content (An_{10}) of albite composition. It covers about 3.4 % of the rock composition (Table 7). Most of plagioclase crystals show albite twinning (Fig. 4, m), but Carlsbad less common twinning. Occasionally, the plagioclase albite twinning is tilted due to deformation. As well as, the albite composition sometimes shows as rim-like surrounded crystals of microcline or perthite to show well developed rapakivi texture. (Fig. 4, m). **Muscovite.** It is represented by euhedral and subhedral flaky crystals. It reaches about 2 mm in length and 1.2 mm in width, and covers about 2% of the rock composition (Table 7). Occasionally, it is partly or completely altered to chlorite particular along the plans of cleavage in banding like shape. It is corroded often by groundmass (Fig. 4, n). **Sphene.** It is represented by prismatic crystals of notably high refractive indices, up to 0.6 mm in length and 0.3 mm in width, is the common accessory mineral, up to 0.4 % of the rock composition (Table 7). It characterized by pale yellow, commonly with grayish-brown shades, slightly pleochroing to pale green and often associating with muscovite aggregates. **Iron oxides** occur as black dots within the rock and between the mineral constituents as shown (Fig. 4, n).

II.5. Dikes. The different types of dikes occur in the study area of composition varying from basic to acidic composition (Table 8). The plotted modal composition of them on QAP diagram of Streckeisen (1976), According to these diagrams they are classified into granitic, andesite, rhyolite and basalt dikes as show (Figs. 5, f, g).

II.5.a. Granitic dikes. They consist of alkalifelspar, plagioclase and muscovite minerals. Iron oxides are the accessory minerals, but biotite is less common as shown in (Fig. 4, o).

II.5.b. Andesite dikes. They consist essentially of plagioclase (58.5%), hornblende (16%) and biotite (10.5%), with few amount of quartz (8.5%). Iron oxides are the accessory minerals as shown in. (Fig. 4, p).

II.5.c. Rhyolite dike. These dikes consist of alkali feldspar (36%), quartz (31%) and plagioclase (23%) composition with minor amount of muscovite. On the other hand, iron oxides are the main accessory minerals as shown in. (Fig. 4, q).

II.5.d. Basalt dikes. These types occur as fine-grained rocks composed mainly of plagioclase (65.3%) and augite (29.35%). Chlorite is the main secondary mineral. The accessory minerals are iron oxides as shown in. (Fig. 4, r).
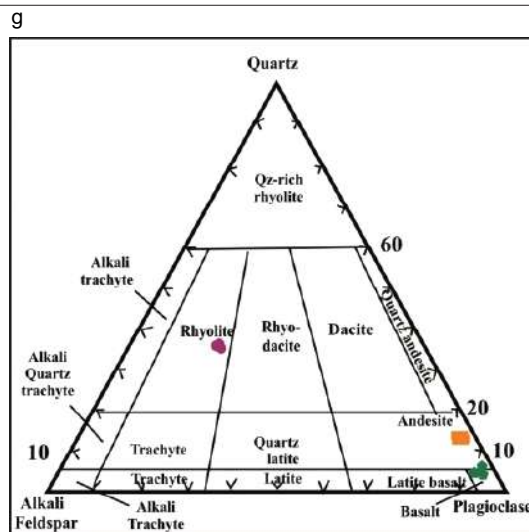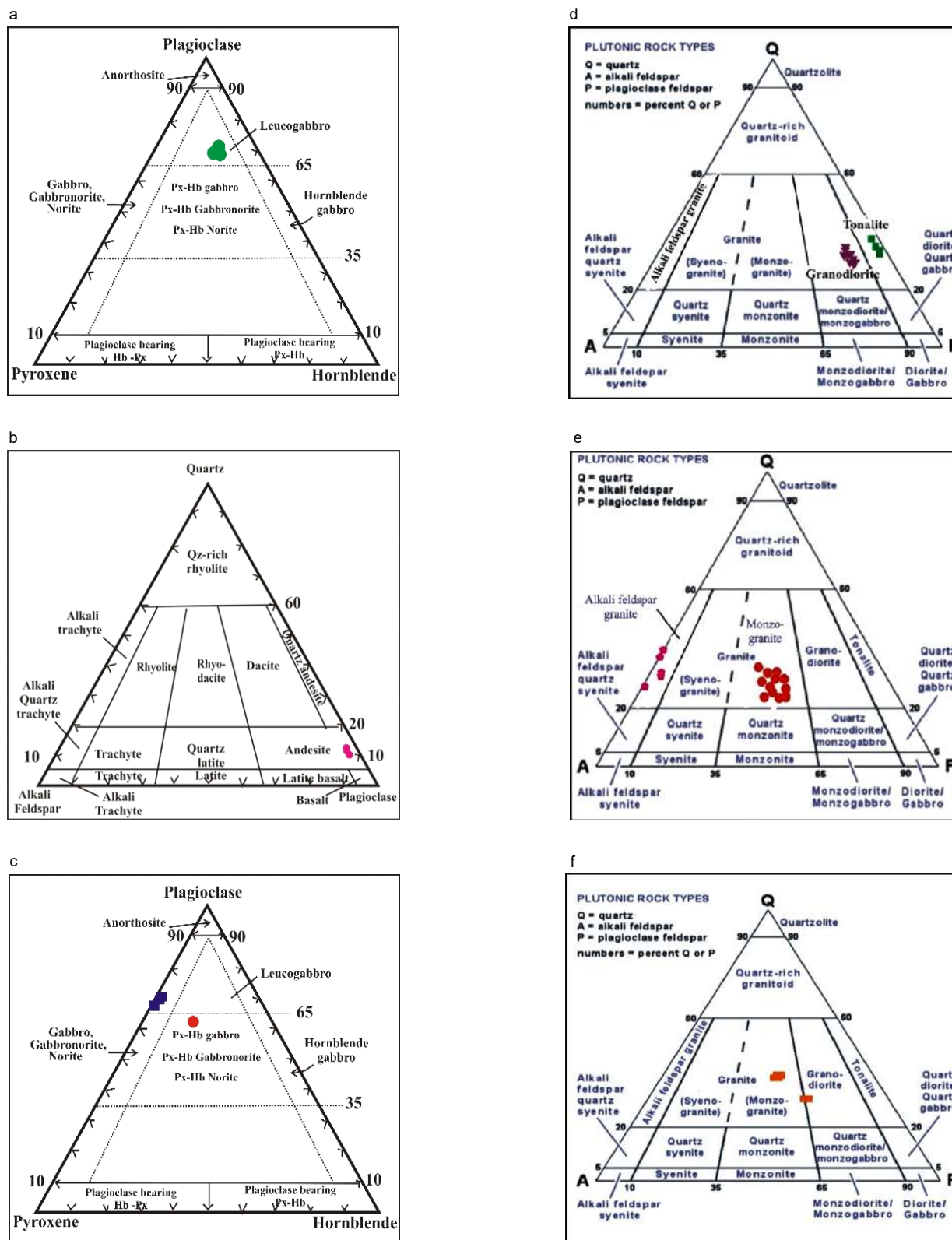
Figure 5. Plot of the investigated metagabbro on IUGS nomenclature for gabbroic rocks of Le Maitre classification diagram, 2002 (a); modal composition of the investigated andesitic rocks on QAP of Streckeisen volcanic classification diagram, 1976 (b); the investigated gabbroic rocks on IUGS nomenclature for gabbroic rocks of Le Maitre classification diagram, 2002 (c); the modal composition of the early orogenic granitic rocks on QAP diagram of Streckeisen, 1976 (d); modal composition of the investigated late orogenic granites on QAP of Streckeisen classification diagram, 1976 (e); QAP of Streckeisen diagram, 1976, for the investigated granitic dikes (f); QAP of Streckeisen classification diagram, 1976, for the study volcanic dikes (g).

Рисунок 5. График исследуемого метагаббро по номенклатуре IUGS для габбро-пород классификации Le Maitre, 2002 (а); модальный состав исследованных андезитовых пород по QAP вулканической классификационной диаграммы Штрекейзена, 1976 (б); исследованные габбро-породы по номенклатуре IUGS для габбро-пород классификации Le Maitre, 2002 (с); модальный состав раннеорогенных гранитных пород на диаграмме QAP Штрекейзена, 1976 (г); модальный состав исследованных позднеорогенных гранитов по QAP классификационной диаграммы Штрекейзена, 1976 (е); QAP диаграммы Штрекейзена, 1976, для исследованных гранитных даек (f); QAP классификационной диаграммы Штрекейзена, 1976 г., для изучения вулканических даек (г).

Conclusion

Um Taghir area is located in the Central Eastern Desert of Egypt on the Qena–Safaga road. The Qena–Safaga shear zone one of the most important structural occurrences in Central Eastern Desert of Egypt. It is dominated by metamorphic complex and they are intruded by granitic rocks. As well as, Um Taghir is represented by island arc related rocks and late to post tectonic magmatism. The island arc related rocks are represented by metavolcaniclastic rocks and metagabbro. Metavolcanoclastic rocks are considered as the older rock units of the study are and intruded by the metagabbro. Whereas the late to post magmatism is represented by (dokhan volcanic, gabbro, tonalite-granodiorite, monzogranite, alkali feldspar granites and different types of dikes). Usually, the gabbroic rock is bearing ilmenite lenses or bands in the bottom of the layered; this is related to magma rich of iron oxides. Petrographically, island arc assemblage is classified in to actinolite hornblende schist and metagabbro that show quite different of their content in plagioclase, hornblende, augite, quartz and biotite. Occasionally, the late to post magmatism represented by (andesite, gabbro, tonalite, granodiorite monzogranite, alkali feldspar granites and different types of dikes). Andesite consists of plagioclase, quartz, alkali feldspar and hornblende. Gabbroic rocks are represented by pyroxene hornblende gabbro and leucogabbro. They show quite different of their content in plagioclase, pyroxene and clear difference in the content of both olivine and hornblende in both of them. While tonalite and granodiorite that show quite different of their content in plagioclase, quartz, hornblende, alkali felspar and biotite. On the other hand, monzogranite and alkali feldspar granite, they show plagioclase is varying from oligoclase to albite; K-feldspars, quartz and muscovite are relatively more abundant in the alkali feldspar granite. Finally, the different types of dikes classified into granite, andesite, rhyolite and basalt dikes consist of the different mineral compositions.

REFERENCES

1. Abdelsalam M. G., Stern R. J. 1996, Sutures and shear zones in the Arabian-Nubian Shield. *Journal of African Earth Sciences*, vol. 23, issue 3, pp. 289–310. https://ui.adsabs.harvard.edu/link_gateway/1996JAfES..23..289A/doi:10.1016/S0899-5362(97)00003-1

2. Abd El-Wahed M. A., Harraz H. Z., El-Behairy M. H. 2016, Transpressional imbricate thrust zones controlling gold mineralization in the Central Eastern Desert of Egypt. *Ore Geol Rev*., vol. 78, pp. 424–446.

3. Abd El-Wahed I. A., Thabet I. A. 2017, Strain geometry, microstructure and metamorphism in the dextral transpressional Mubarak shear belt, Central Eastern Desert. *Egypt Geotectonics*, vol. 51, pp. 438–462.

4. Akaad M. K., El-Gaby S., Habib M. E. 1973, The Barud Gneisses and the origin of Grey Granite. *Bull. Fac. Sci. Assiut Univ*., vol. 2, pp. 55–69.

5. Ali B. H., Wilde S. A., Gabr M. M. A. 2009, Granitoid evolution in Sinai, Egypt, based on precise SHRIMP U–Pb zircon geochronology. *Gondwana Research*, vol. 15, issue 1, pp. 38–48. https://doi.org/10.1016/j.gr.2008.06.009

6. Augland L. E., Andresen A., Boghdady G. Y. 2011, U–Pb ID-TIMS dating of igneous and metaigneous rocks from the El-Sibai area: time constraints on the tectonic evolution of the Central Eastern Desert, Egypt. *Int. J. Earth Sci*., vol. 101, issue 1, pp. 25–37. https://doi.org/10.1007/s00531-011-0653-3

7. Collins A. S., Pisarevsky S. A. 2005, Amalgamating eastern Gondwana: the evolution of the Circum-Indian Orogens. *Earth-Science Reviews*, vol. 71, issues 3-4, pp. 229–270. https://doi.org/10.1016/j.earscirev.2005.02.004

8. El-Bialy M. Z., Omar M. M. 2015, Spatial association of Neoproterozoic continental arc I-type and post-collision a-type granitoids in the Arabian-Nubian Shield: The Wadi Al-Baroud older and younger granites, North Eastern Desert, Egypt. *J. Afr. Earth Sci*., vol. 103, pp.1–29.

9. El-Gaby S., Habib M. S. 1982, Geology of the area southwest of Port Safaga, with special emphasis on the granitic rocks, Eastern Desert, Egypt. *Ann. Geol. Surv. Egypt*, vol. XII, pp. 47–71.

10. El-Gaby S., List F. K., Tahrani R. 1988, Geology, evolution and metallogenesis of the Pan-African belt in Egypt. In: The Pan-African belt of the northeast African and adjacent areas, by S. E-I Gaby and R. O. Greiling (Eds). Earth Evol. Sci. Braunschweig: Vieweg, pp. 17–66.

11. Fowler A.-R., Khaled G. A., Omar S. M., Eliwa H. A. 2006, The significance of gneissic rocks and synmagmatic extensional ductile shear zones of the Barud area for the tectonics of the North Eastern Desert, Egypt. *Journal of African Earth Sciences*, vol. 46, issue 3, pp. 201–220. https://doi.org/10.1016/j.jafrearsci.2006.04.011

12. Gass I. G. 1982, Upper Proterozoic (Pan-African) calc-alkaline magmatism in northeastern Africa and Arabia. In: Andesite and related rocks. R. S. Thorpe (ed.). N. Y.: Wiley and Sons, pp. 591–609.

13. Gahlan H. A., Azer M. K., Asimow P., Al-Kahtany K. 2016, Late Ediacaran post-collisional A-type syenites with shoshonitic affinities, northern Arabian-Nubian Shield: a possible mantle-derived A-type magma. *Arabian Journal of Geosciences*, vol. 9, pp. 1–24.

14. Habib M. E., 1987a. Arc ophiolites in the Pan-African basement between Meatiq and Abu Furad, Eastern Desert, Egypt. *Bull. Fac. Sci. Assiut Univ*., vol. 16, pp. 241–283.

15. Habib M. E., 1987b. Microplate accretion model for the Pan-African basement between Qena–Safaga and Qift–Quseir roads, Egypt. *Bull. Fac. Sci. Assiut Univ*., vol. 16, pp. 199–239.

16. Hamimi Z., Zoheir B. A., Younis M. H. 2015b, Polyphase deformation history of the Eastern Desert tectonic terrane in northeastern Africa. In: XII international conference "New ideas in earth sciences". Moscow, April 2015.

17. Hassan S. M., Ramadan T. M. 2014, Mapping of the late Neoproterozoic Basement rocks and detection of the gold-bearing alteration zones at Abu Marawat-Semna area, Eastern Desert, Egypt using remote sensing data. *Arab. J. Geosci*., vol. 8, issue 7, pp. 4641–4656. https://doi.org/10.1007/s12517-014-1562-0

18. Hume W. F. 1934, The fundamental Precambrian rocks of Egypt and the Sudan. *Geology of Egypt*, vol. 2, part 1. Geol. Surv. of Egypt.

19. Jacobs J., Thomas R. J. 2004, Himalayan-type indenter-escape tectonics model for the southern part of the late Neoproterozoic–early Paleozoic East African-Antarctic Orogen. *Geology*, vol. 32, issue 8, pp. 721–724. https://ui.adsabs.harvard.edu/link_gateway/2004Geo....32..721J/doi:10.1130/G20516.1

20. Johnson P. R., Andresen A., Collins A. S., Fowler T. R., Fritz H., Ghebreab W., Kusky T., Stern R. J. 2011, Late Cryogenian-Ediacaran history of the Arabian-Nubian Shield: a review of depositional, plutonic, structural, and tectonic events in the closing stages of the northern East African Orogen. *Journal of African Earth Sciences*, vol. 61, pp. 167–232. https://doi.org/10.1016/j.jafrearsci.2011.07.003

21. Kröner A., Krüger J., Rashwan A. A. A. 1994, Age and tectonic setting of granitoid gneisses in the Eastern Desert of Egypt and south-west Sinai. *Geologische Rundschau*, vol. 83, issue 3, pp. 502–513. https://doi.org/10.1007/bf01083223

22. Le Maitre R. W. 2002, Igneous rocks – a classification and glossary of terms. Recommendations of the IUGS subcommission on the Systematics of Igneous Rocks. 2nd edition. Cambridge: Cambridge University Press. 236 p. https://doi.org/10.1017/CBO9780511535581

23. Makroum F. 2017, Structural Interpretation of the Wadi Hafafit Culmination: a pan-African gneissic dome in the central Eastern Desert, Egypt. *Lithosphere*, vol. 9, issue 5, pp. 759–773. https://doi.org/10.1130/L645.1

24. Shalaby A., Stüwe K., Makroum F., Frtiz H., Kebede T., Klötzli U. 2005, The Wadi Mubarak belt, Eastern Desert of Egypt: a Neoproterozoic conjugate shear system in the Arabian-Nubian Shield. *Precambrian Research*, vol. 136, issue 1, pp. 27–50. https://doi.org/10.1016/j.precamres.2004.09.005

25. Stern R. J. 1994, Arc assembly and continental collision in the Neoproterozoic East African Orogen: implications for the consolidation of

Gondwanaland. *Annual Reviews of Earth and Planetary Sciences*, vol. 22, pp. 319–351. http://dx.doi.org/10.1146/annurev.ea.22.050194.001535
26. Stoeser D. B., Frost C. D. 2006, Nd, Pb, Sr, and O isotopic characterization of Saudi Arabian Shield terranes. *Chemical Geology*, vol. 226, issues 3-4, pp. 163–188. https://doi.org/10.1016/j.chemgeo.2005.09.019
27. Streckeisen A. 1976, Plutonic rocks: Classification and nomenclature recommended by the IVGS sub-commission on the systematic of igneous rocks. *Geotims.*, vol. 18, pp. 26–30.

The article was received on November 15, 2019

УДК 551.24 : 552.08 : 552.3 + 552.4

Геологические и петрографические исследования в районе Ум Тагир Центральной части Восточной пустыни, Египет

Хамди Ахмед Мохамед АВАД,
Алексей Валерьевич НАСТАВКИН

Южный федеральный университет, Ростов-на-Дону, Россия

Аннотация

Район Ум Тагир расположен на северной крайней границе Средне-Восточной пустыни Египта на западе города Сафага. Ум Тагир представлен скалами, связанными с островной дугой и поздним тектоническим магматизмом. Горные породы, связанные с островной дугой, представлены метавулканическими пластами и метагаббровыми породами. Метавулканокластические породы считаются более старыми литологическими единицами исследования интрудируемые метагаббро. От позднего до посттектонического магматизма представлены вулканиты доханской свиты, габбро, тоналит- гранодиорит, монцогранит, щелочной полевой шпат и различные типы даек. Как правило, габбровая порода является носителем ильменитовых линз или полос в нижней части слоистых слоев; это связано с магмой, богатой оксидами железа. ***Петрографически,*** состав островной дуги подразделяется на актинолит-роговообманковый сланец и метагаббро, что присутствует в разных значениях в плагиоклазе, роговой обманке, авгите, кварце и биотите. Изредка поздний и тектонический магматизм представлен андезитом, габбро, тоналитом, гранодиоритом, монцогранитом, щелочно-полевошпатовым гранитом и различными типами даек. Андезит состоит из плагиоклаза, кварца, щелочного полевого шпата и роговой обманки. Габбровые породы представлены пироксеновыми роговыми обманками габбро и лейкогаббро. Они присутствуют в разном содержании в плагиоклазе, пироксене и демонстрируют явные разногласия в содержании, как оливина, так и роговой обманки у обоих из указанных. В то время как тоналит и гранодиорит присутствуют в довольно разных значениях в плагиоклазе, кварце, роговой обманке, щелочном полевом шпате и биотите. С другой стороны, монцогранит и щелочно-полевошпатовый гранит показывают, что плагиоклаз варьируется от олигоклаза до альбита; К-полевые шпаты, кварц и мусковит относительно более распространены в щелочном полевом шпате. Наконец, различные типы даек, классифицированных как гранитные, андезитовые, риолитовые и базальтовые дайки; они состоят из различных минеральных составов.

Ключевые слова: район Ум Тагир, петрография, Восточная пустыня, Египет.

ЛИТЕРАТУРА
1. Abdelsalam M. G., Stern R. J. 1996, Sutures and shear zones in the Arabian-Nubian Shield. *Journal of African Earth Sciences*, vol. 23, issue 3, pp. 289–310. https://ui.adsabs.harvard.edu/link_gateway/1996JAfES..23..289A/doi:10.1016/S0899-5362(97)00003-1
2. Abd El-Wahed M. A., Harraz H. Z., El-Behairy M. H. 2016, Transpressional imbricate thrust zones controlling gold mineralization in the Central Eastern Desert of Egypt. *Ore Geol Rev.*, vol. 78, pp. 424–446.
3. Abd El-Wahed I. A., Thabet I. A. 2017, Strain geometry, microstructure and metamorphism in the dextral transpressional Mubarak shear belt, Central Eastern Desert. *Egypt Geotectonics*, vol. 51, pp. 438–462.
4. Akaad M. K., El-Gaby S., Habib M. E. 1973, The Barud Gneisses and the origin of Grey Granite. *Bull. Fac. Sci. Assiut Univ.*, vol. 2, pp. 55–69.
5. Ali B. H., Wilde S. A., Gabr M. M. A. 2009, Granitoid evolution in Sinai, Egypt, based on precise SHRIMP U–Pb zircon geochronology. *Gondwana Research*, vol. 15, issue 1, pp. 38–48. https://doi.org/10.1016/j.gr.2008.06.009
6. Augland L. E., Andresen A., Boghdady G. Y. 2011, U–Pb ID-TIMS dating of igneous and metaigneous rocks from the El-Sibai area: time constraints on the tectonic evolution of the Central Eastern Desert, Egypt. *Int. J. Earth Sci.*, vol. 101, issue 1, pp. 25–37. https://doi.org/10.1007/s00531-011-0653-3
7. Collins A. S., Pisarevsky S. A. 2005, Amalgamating eastern Gondwana: the evolution of the Circum-Indian Orogens. *Earth-Science Reviews*, vol. 71, issues 3-4, pp. 229–270. https://doi.org/10.1016/j.earscirev.2005.02.004
8. El-Bialy M. Z., Omar M. M. 2015, Spatial association of Neoproterozoic continental arc I-type and post-collision a-type granitoids in the Arabian-Nubian Shield: The Wadi Al-Baroud older and younger granites, North Eastern Desert, Egypt. *J. Afr. Earth Sci.*, vol. 103, pp.1–29.
9. El-Gaby S., Habib M. S. 1982, Geology of the area southwest of Port Safaga, with special emphasis on the granitic rocks, Eastern Desert, Egypt. *Ann. Geol. Surv. Egypt*, vol. XII, pp. 47–71.
10. El-Gaby S., List F. K., Tahrani R. 1988, Geology, evolution and metallogenesis of the Pan-African belt in Egypt. In: The Pan-African belt of the northeast African and adjacent areas, by S. E-I Gaby and R. O. Greiling (Eds). Earth Evol. Sci. Braunschweig: Vieweg, pp. 17–66.
11. Fowler A.-R., Khaled G. A., Omar S. M., Eliwa H. A. 2006, The significance of gneissic rocks and synmagmatic extensional ductile shear zones of the Barud area for the tectonics of the North Eastern Desert, Egypt. *Journal of African Earth Sciences*, vol. 46, issue 3, pp. 201–220. https://doi.org/10.1016/j.jafrearsci.2006.04.011
12. Gass I. G. 1982, Upper Proterozoic (Pan-African) calc-alkaline magmatism in northeastern Africa and Arabia. In: Andesite and related rocks. R. S. Thorpe (ed.). N. Y.: Wiley and Sons, pp. 591–609.
13. Gahlan H. A., Azer M. K., Asimow P., Al-Kahtany K. 2016, Late Ediacaran post-collisional A-type syenites with shoshonitic affinities, northern Arabian-Nubian Shield: a possible mantle-derived A-type magma. *Arabian Journal of Geosciences*, vol. 9, pp. 1–24.

✉hamdiawaad@gmail.com
ⓘ https://orcid.org/0000-0001-5306-8015
ⓘ https://orcid.org/0000-0003-1472-9399

14. Habib M. E., 1987a. Arc ophiolites in the Pan-African basement between Meatiq and Abu Furad, Eastern Desert, Egypt. *Bull. Fac. Sci. Assiut Univ.*, vol. 16, pp. 241–283.

15. Habib M. E., 1987b. Microplate accretion model for the Pan-African basement between Qena–Safaga and Qift–Quseir roads, Egypt. *Bull. Fac. Sci. Assiut Univ.*, vol. 16, pp. 199–239.

16. Hamimi Z., Zoheir B. A., Younis M. H. 2015b, Polyphase deformation history of the Eastern Desert tectonic terrane in northeastern Africa. In: XII international conference "New ideas in earth sciences". Moscow, April 2015.

17. Hassan S. M., Ramadan T. M. 2014, Mapping of the late Neoproterozoic Basement rocks and detection of the gold-bearing alteration zones at Abu Marawat-Semna area, Eastern Desert, Egypt using remote sensing data. *Arab. J. Geosci.*, vol. 8, issue 7, pp. 4641–4656. https://doi.org/10.1007/s12517-014-1562-0

18. Hume W. F. 1934, The fundamental Precambrian rocks of Egypt and the Sudan. *Geology of Egypt*, vol. 2, part 1. Geol. Surv. of Egypt.

19. Jacobs J., Thomas R. J. 2004, Himalayan-type indenter-escape tectonics model for the southern part of the late Neoproterozoic–early Paleozoic East African-Antarctic Orogen. *Geology*, vol. 32, issue 8, pp. 721–724. https://ui.adsabs.harvard.edu/link_gateway/2004Geo....32..721J/doi:10.1130/G20516.1

20. Johnson P. R., Andresen A., Collins A. S., Fowler T. R., Fritz H., Ghebreab W., Kusky T., Stern R. J. 2011, Late Cryogenian-Ediacaran history of the Arabian-Nubian Shield: a review of depositional, plutonic, structural, and tectonic events in the closing stages of the northern East African Orogen. *Journal of African Earth Sciences*, vol. 61, pp. 167–232. https://doi.org/10.1016/j.jafrearsci.2011.07.003

21. Kröner A., Krüger J., Rashwan A. A. A. 1994, Age and tectonic setting of granitoid gneisses in the Eastern Desert of Egypt and south-west Sinai. *Geologische Rundschau*, vol. 83, issue 3, pp. 502–513. https://doi.org/10.1007/bf01083223

22. Le Maitre R. W. 2002, Igneous rocks – a classification and glossary of terms. Recommendations of the IUGS subcommission on the Systematics of Igneous Rocks. 2nd edition. Cambridge: Cambridge University Press. 236 p. https://doi.org/10.1017/CBO9780511535581

23. Makroum F. 2017, Structural Interpretation of the Wadi Hafafit Culmination: a pan-African gneissic dome in the central Eastern Desert, Egypt. *Lithosphere*, vol. 9, issue 5, pp. 759–773. https://doi.org/10.1130/L645.1

24. Shalaby A., Stüwe K., Makroum F., Frtiz H., Kebede T., Klötzli U. 2005, The Wadi Mubarak belt, Eastern Desert of Egypt: a Neoproterozoic conjugate shear system in the Arabian-Nubian Shield. *Precambrian Research*, vol. 136, issue 1, pp. 27–50. https://doi.org/10.1016/j.precamres.2004.09.005

25. Stern R. J. 1994, Arc assembly and continental collision in the Neoproterozoic East African Orogen: implications for the consolidation of Gondwanaland. *Annual Reviews of Earth and Planetary Sciences*, vol. 22, pp. 319–351. http://dx.doi.org/10.1146/annurev.ea.22.050194.001535

26. Stoeser D. B., Frost C. D. 2006, Nd, Pb, Sr, and O isotopic characterization of Saudi Arabian Shield terranes. *Chemical Geology*, vol. 226, issues 3-4, pp. 163–188. https://doi.org/10.1016/j.chemgeo.2005.09.019

27. Streckeisen A. 1976, Plutonic rocks: Classification and nomenclature recommended by the IVGS sub-commission on the systematic of igneous rocks. *Geotims.*, vol. 18, pp. 26–30.